Magnetic Properties of Nickel Filament Polymer-Matrix Composites

XIAOPING SHUI and D.D.L. CHUNG

Composite Materials Research Laboratory, State University of New York at Buffalo, Buffalo, NY 14260-4400

The magnetic properties of polyethersulfone-matrix composites with 3–19 vol.% polycrystalline nickel filaments (0.4 μm diam) were investigated. These filaments were found to exhibit hysteresis energy loss 10800 J/m³ of nickel and coercive force 16.9 kA/m, compared to corresponding values of 4930 J/m³ and 4.7 kA/m for 2 μm diam polycrystalline nickel fibers, 1020 J/m³ and 0.5 kA/m for 20 μm diam polycrystalline nickel fibers, and 1280 J/m³ and 2.3 kA/m for solid polycrystalline nickel.

Keywords: Composite, fibers, filaments, hysteresis energy loss, magnetic, nickel, polymer

INTRODUCTION

Magnetic materials in discontinuous forms (such as particles and short fibers) are used as fillers in polymers[1–7] and other matrices[8–10] for producing magnetic composite materials that are low in both cost and eddy-current energy loss. However, the magnetic properties of discontinuous magnetic materials have received little attention compared to those of continuous magnetic materials. Even less attention has been given to magnetic fibers than magnetic particles. Due to the large aspect ratio, discontinuous fibers have more chance than particles at the same volume fraction to touch one another, so fibers are more effective than particles in serving as a filler. This paper provides a study of the magnetic properties of discontinuous nickel fibers or filaments of various diameters, in comparison to those of solid nickel.

Nickel filaments of diameter 0.4 μm have been recently shown to be a highly effective filler for providing polymer-matrix composites with high electromagnetic interference (EMI) shielding effectiveness.[11] A shielding effectiveness of 87 dB (1–2 GHz) was attained with just 7 vol.% nickel filaments in a polymer-matrix composite of thickness 2.8 mm.[11] Magnetic properties are relevant to the shielding ability, but have not been previously reported on these composites. The objective of this work is to investigate the magnetic properties of nickel filament polymer-matrix composites.

(Received October 23, 1995; revised January 2, 1996)

EXPERIMENTAL METHODS

The nickel filaments (0.4 μm in diam, >100 μm in length) and composite fabrication (with polyether sulfone or PES as the matrix) were described in Ref. 1. Each nickel filament had a carbon filament core of diameter ~0.1 μm, as illustrated in Fig. 1, because a nickel filament was fabricated by the electroplating of nickel onto a carbon filament. The nickel filaments had a bent morphology, resembling cotton wool, as shown by the scanning electron microscope photographs of Fig. 2. The filaments were randomly oriented in the composites.

The nickel fibers used for comparing with the nickel

filaments were

- 2 μm in diameter and 2000 μm in length, as provided by Ribtec (Gahanna, Ohio), and
- 20 μm in diameter and 1000 μm in length, as provided as Fibrex by National-Standard Co. (Corbin, KY).

Due to the large length of the nickel fibers of diameter 2 μm (which resemble cotton wool), the dispersion of these fibers was most difficult.

The composites were fabricated by forming a dry mixture of the polymer powder and the filler and subsequent hot pressing in a steel mold at 310°C (processing temperature for PES, as recommended by ICI, the manufacturer) and 13.4 MPa for ~30 min. For the nickel filaments and the 20 μm diam Ni fibers, the mixing was carried out dry in a ball mill. For the 2 μm diam nickel fibers, mixing was performed by hand, as neither the above-mentioned dry mixing nor wet (blender) mixing was possible.

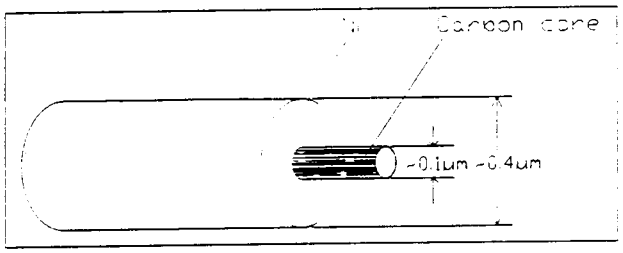

Fig. 1. Schematic illustration of a nickel filament.

The intrinsic magnetic induction (B_i), which is equal to $\mu_0 M$ (where M is the magnetization), was measured as a function of the magnetic field strength (H), thereby obtaining the B-H hysteresis loop, at room temperature using a Quantum Design SQUID magnetometer. The magnetic moment sensitivity was 10^{-5} emu G. The sample volume was 6.2 mm^3. The measurement involved

- magnetizing the sample at a preset H,
- moving the sample by 4 cm axially inside a coil and measuring the current induced in the coil,
- calculating the magnetic moment, which is related to B_i.

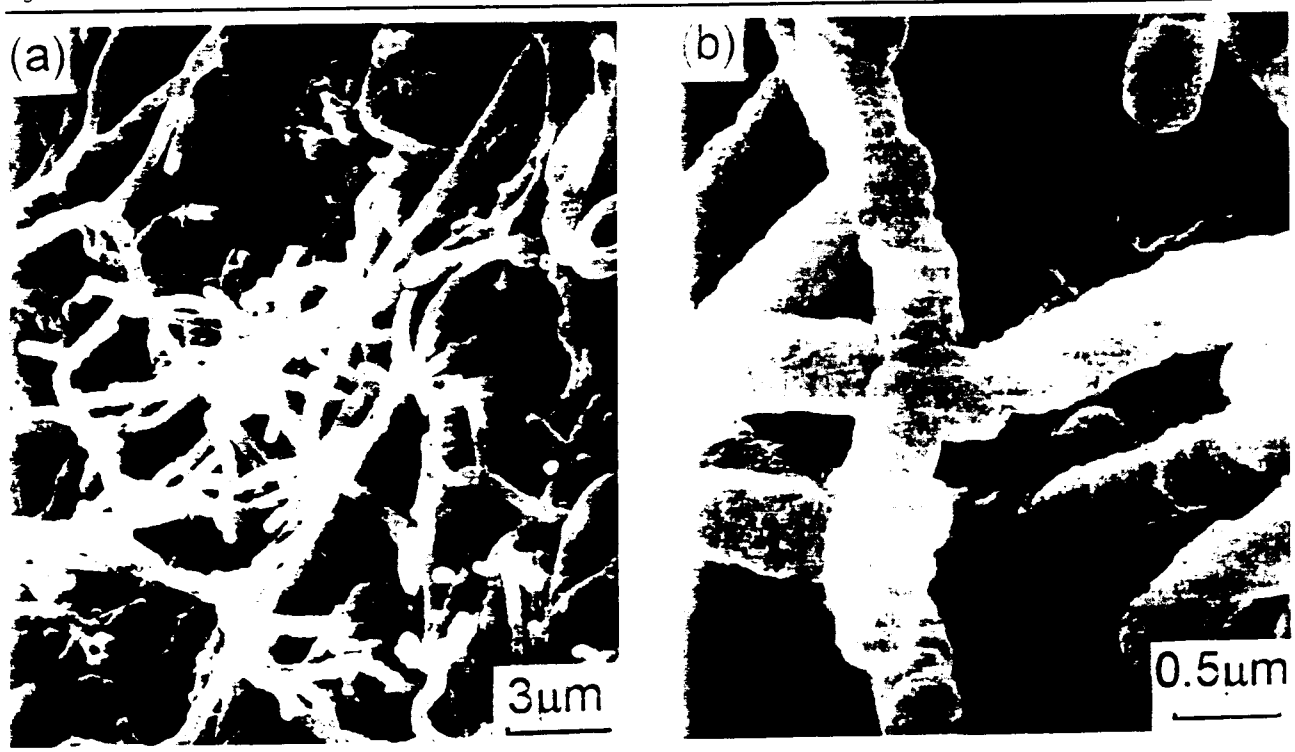

Fig. 2. Scanning electron microscope photographs at two different magnifications of nickel filaments. (From: Ref. 1).

Table I. Magnetic Properties with Respect to Whole Samples

Filler Vol.%	Filler Diam (μm)	$B_{i,m}$ (T)	$B_{i,r}$ (T)	$B_{i,r}/B_{i,m}$	H_c (kA/m)	Hysteresis Energy Loss (J/m^3)
3	0.4	0.0121	3.3×10^{-3}	0.27	16.8	309
7	0.4	0.0298	7.6×10^{-3}	0.26	16.8	714
13	0.4	0.0555	1.5×10^{-2}	0.27	16.9	1406
19	0.4	0.0674	1.4×10^{-2}	0.21	15.9	1400
19	2	0.106	1.1×10^{-2}	0.10	4.65	936
19	20	0.132	1.3×10^{-3}	9.84×10^{-3}	0.45	193
Solid Ni		0.616	8.8×10^{-3}	1.43×10^{-2}	2.25	1283

This procedure was repeated at each H value from 0 to +x, then from +x to –x, then from –x to +x and then from +x to 0, where x = 238.7 kA/m and x = 40 kA/m (i.e., two B_i-H loops) for each sample, such that nearest H values were 4 kA/m apart.

The grain size was measured by x-ray diffraction, using CuK_α radiation and the 20 μm diam nickel fibers as the standard.

RESULTS AND DISCUSSION

Tables I and II and Figs. 3–6 give the magnetic behavior of various nickel composites and solid nickel. Table I and Fig. 3 and Fig. 5 give B_i of the composites, whereas Table II and Fig. 4 and Fig. 6 give B_i when only the nickel part of each sample was considered. The B_i of each composite (Table I and Fig. 3 and Fig. 5) was divided by the volume fraction of nickel in the composite to obtain the B_i of the composite when only the nickel part of each sample was considered (Table II and Fig. 4 and Fig. 6). Figures 3, 4, 5a, and 6a only show the portion between –40 and +40 kA/m; at H greater than +40 kA/m, B continued to increase, as shown in Fig. 5b and 6b; $B_{i,m}$ (maximum B_i) in Tables I and II was arbitrarily taken as the B_i value at H = 238.7 kA/m.

$B_{i,m}$ increased with increasing volume fraction of nickel filaments from 3 to 19% (Table I). When only the nickel part of the sample was considered, $B_{i,m}$ was the same for nickel filament volume fractions of 3, 7, and 13%, but was slightly smaller at 19 vol.% (Table II). $B_{i,m}$ of the sample as well as $B_{i,m}$ when only the nickel part of the sample was considered, increased with increasing filler diameter (0.4, 2, and 20 μm) at a fixed filler volume fraction (19%). The trends concerning $B_{i,m}$ when only the nickel part of the sample was considered mean that the ease of magnetization was quite independent of the filament volume fraction, but increased with increasing filament diameter.

The ratio of $B_{i,r}$ (remanent B_i) to $B_{i,m}$ when only the nickel part of the sample was considered was comparably large for nickel filaments at 3, 7, 13, and 19 vol.%, and decreased with increasing filler diameter at a constant filler content of 19 vol.%. The H_c (coercive force) was comparably large for nickel filaments at 3, 7, 13, and 19 vol.%, and decreased sharply with increasing filler diameter at a constant filler content of 19 vol.%. These trends of $B_{i,r}$ and H_c indicate that the ease of demagnetization was independent of the filament volume fraction and increased sharply with increasing filler diameter.

The hysteresis energy loss per m^3 of nickel (Table II) was comparably large for nickel filaments at 3, 7, and 13 vol.%, but was lower at 19 vol.%. At a fixed filler content of 19 vol.%, the hysteresis energy loss per m^3

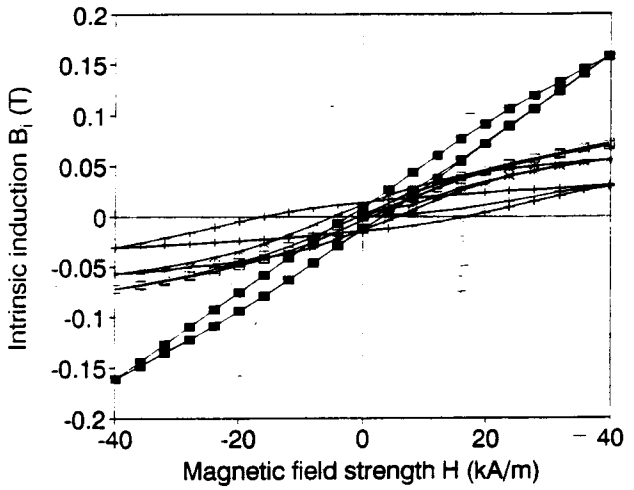

Fig. 3. B-H loops for solid nickel (■) and composites with 19 vol.% nickel of diameter 0.4 μm (+), 2 μm (*) and 20 μm ( ). B was obtained by considering the whole of each sample.

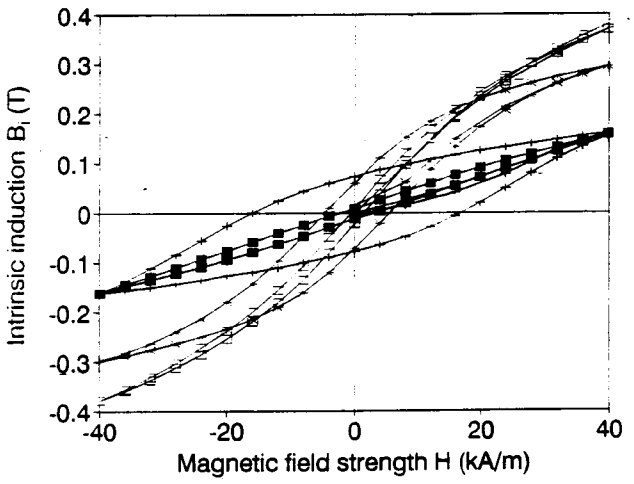

Fig. 4. B-H loops for solid nickel (■) and composites with 19 vol.% nickel of diameter 0.4 μm (+), 2 μm (*) and 20 μm ( ). B was obtained by considering only the nickel part of each sample.

Table II. Magnetic Properties with Respect to the Nickel Part of Each Sample

Filler Vol.%	Filler Diam (μm)	$B_{i,m}$ (T)	$B_{i,r}$ (T)	$B_{i,r}/B_{i,m}$	H_c (kA/m)	Hysteresis Energy Loss (J/m³)
3	0.4	0.403	0.109	0.27	16.8	10300
7	0.4	0.426	0.108	0.26	16.8	10200
13	0.4	0.427	0.116	0.27	16.9	10815
19	0.4	0.355	0.074	0.21	15.9	7368
19	2	0.558	0.060	0.10	4.65	4926
19	20	0.695	6.7×10^{-3}	9.84×10^{-3}	0.45	1016
Solid Ni		0.616	8.8×10^{-3}	1.43×10^{-2}	2.25	1283

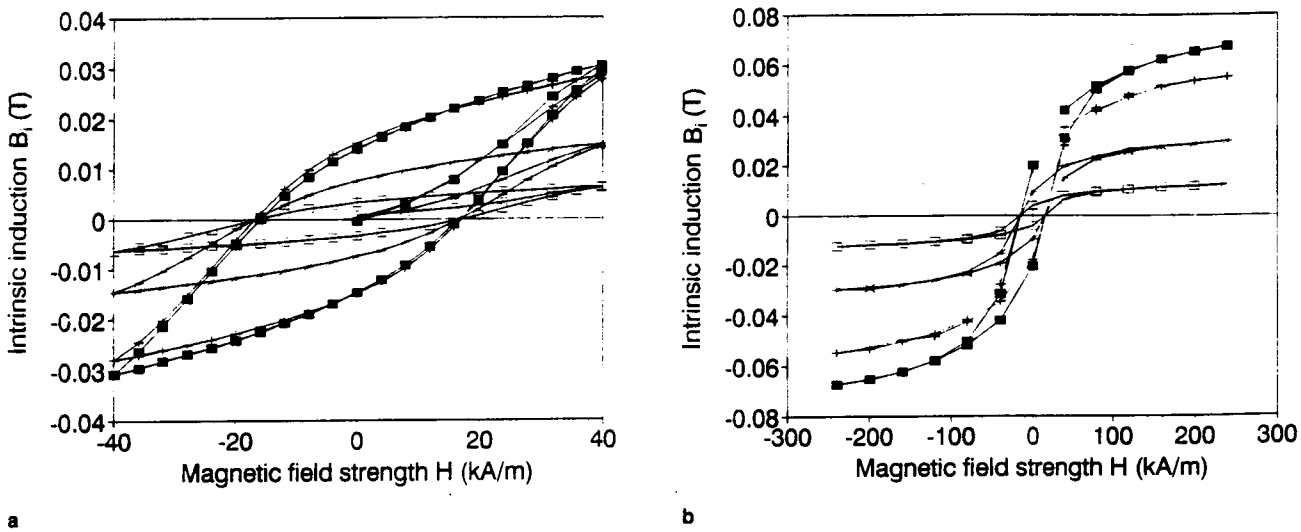

Fig. 5. B-H loops for composites with 0.4 μm diam nickel filaments at 3 vol.% ( ), 7 vol.% (*), 13 vol.% (+), and 19 vol.% (■). B was obtained by considering the whole of each sample. (a) H between −40 and +40 kA/m; (b) H between −250 and +250 kA/m.

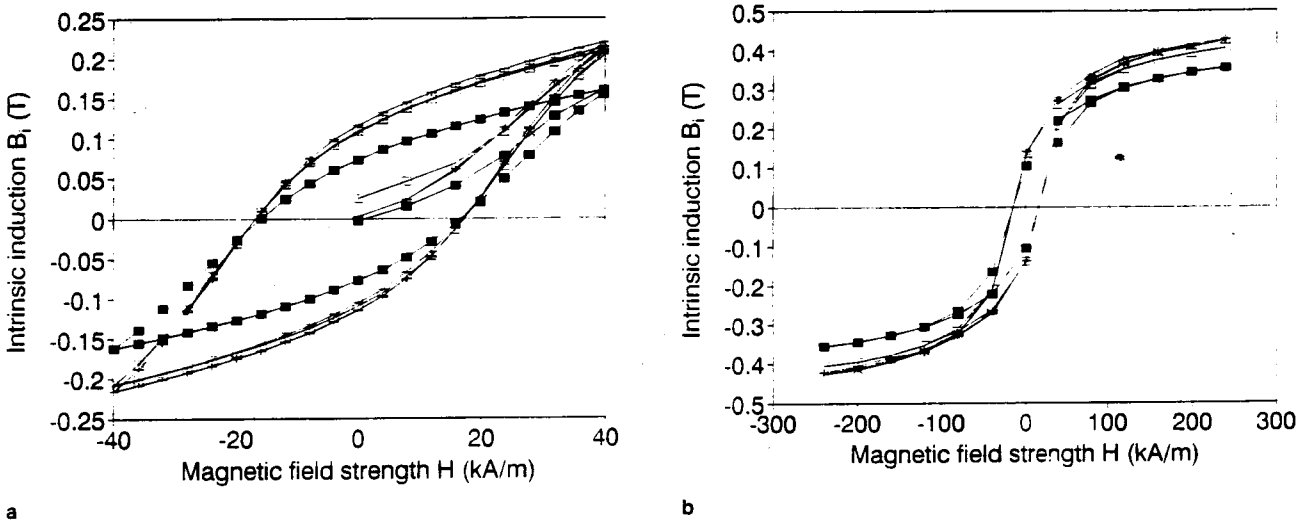

Fig. 6. B-H loops for composites with 0.4 μm diam nickel filaments at 3 vol.% ( ), 7 vol.% (*), 13 vol.% (+), and 19 vol.% (■). B was obtained by considering only the nickel part of each sample. (a) H between −40 and +40 kA/m; (b) H between −250 and +250 kA/m.

of nickel decreased with increasing filler diameter. The B_{i_f}/B_{i_m} ratio was also lower at 19 vol.% than the other filament contents. The observed hysteresis loss is attributed to the difficulty of domain boundary movement and/or the eddy current loss. The observed loss was greatly decreased by increasing the filler diameter, i.e., decreasing the phase boundary concentration (which in turn inhibits domain boundary movement) and enhancing percolation (which in turn enhances eddy current loss). The observed loss was slightly enhanced by increasing the filament content from 13 to 19 vol.%, i.e., decreasing the phase boundary (nickel-polymer interface) concentration and enhancing percolation.

Table III gives the grain size of the nickel filaments and fibers of various diameters, as estimated from the full-width-at-half-maximum of the 111 nickel peak at $2\theta = 44.61°$. Figure 7 shows the x-ray diffraction pattern of the 0.4 μm diam nickel filaments. The grain size is much smaller for the fibers of diameter 2 μm and the filaments of diameter 0.4 μm than the fibers of diameter 20 μm. For all fibers and filaments, the grain size is much smaller than the filler diameter. In spite of the small diameter, the 0.4 μm diam filaments have an average of nine grains between the outer phase boundary adjacent to the polymer and the inner phase boundary adjacent to the carbon core. However, the average number of grains across a diameter is even higher for the 2 μm diam fibers.

DC volume electrical resistivity measurement of composites showed that the resistivity was 5.0×10^{-1}, 2.2×10^{-2}, 3.5×10^{-3}, and 1.5×10^{-3} Ω.cm at 3, 7, 13, and 19 vol.% filaments, respectively.[11] Since the resistivity was comparable at 13 and 19 vol.%, the volume fraction of 19% was beyond the percolation threshold. The touching of adjacent filaments at 19 vol.% served to replace some phase boundaries (i.e., nickel-polymer boundaries) by boundaries approaching grain

boundaries (i.e., filament-filament boundaries), thereby enhancing the ease of domain boundary movement and/or eddy current.

DC volume resistivity measurement was also made on filament compacts, as single filament resistivity measurement was impossible due to the small diameter of the filaments. Because of the contact resistance between the filaments in a compact, the compact's resistivity cannot be simply related to the filament's volume resistivity. Nevertheless, the compact resistivities (after mathematical correction) suggest that the nickel filaments are comparable in volume resistivity to the 2 μm diam nickel fibers, but lower than the 20 μm diam nickel fibers.[12]

The hysteresis energy loss increases with decreasing filler diameter, while the EMI shielding effectiveness also increases with decreasing filler diameter.[11] This means that the magnetic hysteresis energy loss contributes to the absorption of EMI, so that the high EMI shielding effectiveness of the 0.4 μm diam nickel filaments is not just due to the skin depth effect, which makes a filler with a small diameter more effective for shielding.

CONCLUSION

Polyethersulfone-matrix composites with 3–19 vol.% polycrystalline nickel filaments (0.4 μm diam) were compared with those with 19 vol.% polycrystalline nickel fibers (2 μm and 20 μm diam). The 0.4 μm diam nickel filaments were found to exhibit hysteresis energy loss 10800 J/m^3 of nickel and coercive force 16.9 kA/m, compared to corresponding values of 4930 J/m^3 and 4.7 kA/m for 2 μm diam nickel fibers, 1020 J/m^3 and 0.5 kA/m for 20 μm diam nickel fibers, and 1280 J/m^3 and 2.3 kA/m for solid nickel. The high hysteresis loss for the 0.4 μm diam nickel filaments is attributed to eddy current loss and/or difficulty of domain boundary movement.

ACKNOWLEDGMENT

The authors appreciate Professor M.J. Naughton of the State University of New York at Buffalo for stimulating discussions. This work was supported by Department of Navy (SBIR program) via Applied Sciences, Inc. and by the Center for Electronic and Electro-Optic Materials of the State University of New York at Buffalo.

Table III. Grain Size of the Nickel Fillers

Filler Diam (μm)	Grain Size (μm)	No. of Grains Between Phase Boundaries
20	2	10
2	0.018	110
0.4	0.016	9

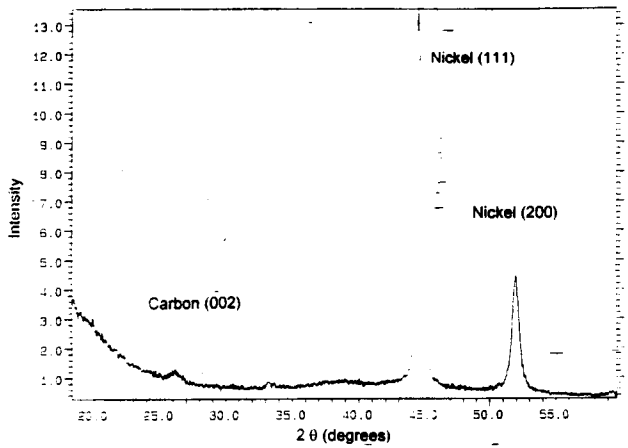

Fig. 7. X-ray diffraction pattern of 0.4 μm diam nickel filaments.

REFERENCES

1. D.R. Saini, V.M. Nadkarni, K.D.P. Nigam and P.D. Grover, *J. Comp. Mater.* 21 (9), 782 (1987).
2. Rina Tannenbaum, Cindy L. Flenniken and Eugene P. Goldberg, *J. Polym. Sci., Part B: Polym. Phys.* 28 (12), 2421 (1990).
3. Zvi Rigbi and Leif Jilken, *J. Magn. Mater.* 37(3), 267 (1983).
4. T. Arivoli, K. Ramkumar and M. Satyam, *J. Phys. D: Appl. Phys.* 21 (4), 636 (1988).
5. Junzo Otera, Tsutomu Makimoto, Wataru Shinoda and Norihisa Hattori, U.S. Patent 4,126,567 (1978).
6. O'Dae Kwon and Jitka Solc, U.S. Patent 4,824,587 (1989).
7. Yukio Ikenaga, Katsuhiko Takahashi, Tsuneyoshi Okada, Kenji Hijikata and Toshio Kanoe, U.S. Patent 4,626,371 (1986).
8. Mutsumi Abe, Ken-ichi Aota and Takashi Motoda, *KOBELCO Technol. Review* 8, 1 (1990).
9. Edward O. Fuchs and James H. Swisher, U.S. Patent 3,647,573 (1972).
10. Chia-Ling Chien, Gang Xiao and Sy-Hwang Liou, U.S. Patent 4,973,525 (1990).
11. Xiaoping Shui and D.D.L. Chung, *J. Electron. Mater.* 24 (2), 107 (1995).
12. Xiaoping Shui, Ph.D. dissertation, State University of New York at Buffalo, 1996.